

PHOTONEUTRON AND TOTAL CROSS-SECTIONS
OF U^{238} IN GIANT RESONANCE

H. G. de Carvalho and J. Benuzzi Martins
Centro Brasileiro de Pesquisas Físicas
Rio de Janeiro - Brazil

V. Di Napoli, D. Margadonna and F. Salvetti
Istituto di Chimica Generale ed Inorganica
dell'Università - Roma

(Received November 27, 1969)

ABSTRACT

From the photofission cross-section; from the (γ, n) cross-section per equivalent quantum, measured at 1000 MeV and from the electric quadrupole moment, the total cross-section of the U^{238} , for photon absorption in the giant resonance, was obtained. The cross-sections for (γ, n) , $(\gamma, 2n)$ and (γ, N) processes are given.

The maximum value of the $\sigma(\gamma, n)$ is 400 mb at 11 MeV with a width $\Gamma(\gamma, n)$ of 2 MeV. The maximum value of the $\sigma(\gamma, \text{total})$ first peak has a value of 470 mb at 11 MeV and the maximum of $\sigma(\gamma, \text{total})$ second peak has a value of 520 mb at 14 MeV. The integrated (γ, total) cross-section is 3.33 MeV-barn in good agreement with the Sum Rule of Thomas-Reiche-Kuhn. The values of nuclear symmetry energy K , obtained by two methods are 28.2 MeV and 23.6 MeV, respectively. The first is in excellent agreement with the average value of 27.4 MeV found by Bramblett et al. and the second with the 23 MeV based in Green's evaluation. The curve of $\sigma(\gamma, 2n)$ is in good agreement with the theoretical curve of Weisskopf for a level density parameter of 20 MeV^{-1} .

The (γ, N) cross-section has a maximum value of 1236 mb at 14 MeV and a $\Gamma(\gamma, N)$ value of 6.0 MeV.

1. INTRODUCTION

The total cross-section of U^{238} has never been accurately measured for photon absorption in the giant resonance. From the photofission cross-section, the (γ, n) cross-section per equivalent quantum of U^{238} measured at 1000 MeV ^{1, 2} and from the electric quadrupole moment ³, we were able to calculate the (γ, n) , the $(\gamma, 2n)$, the (γ, total) and the (γ, N) cross-sections.

The general features of the giant resonance have been explained with about equal success using either the assumption of strong, long-range correlations or no correlations at all, in the excited state ^{4, 5}. The first is usually called the hydrodynamic model and the latter, the shell-model approach. A connection between these different starting point has been pointed out by Brink ⁶, who showed that in an independent-particle model harmonic-oscillator potential, the state of the nucleus after photon absorption actually corresponds to the motion of all protons in regard to neutrons, in accordance with the third model postulated by Goldhaber and Teller. ⁷

Absorption of dipole radiation in the nucleus has been treated as a hydrodynamical problem by Steinwedel and Jensen ⁴. We shall restrict ourselves simply to their point of view and furthermore we shall disregard the compressibility of nuclear matter and the Coulomb repulsion of protons. It can be assumed that the surface is rigid, since surface oscillations do not

couple with the monopole and dipole modes ⁸, although they couple strongly with the quadrupole and higher modes. Errors introduced by the above approximation are small. The Lorenz line expression used to fit the shape of the cross-section curve for photon absorption is given by:

$$\sigma = \frac{\sigma_0}{(E^2 - E_0^2)^2 + \frac{\Gamma^2 E^2}{1}} \quad (1)$$

where σ_0 denotes the peak cross-section at energy E_0 , E is the energy of the external field, and Γ is the full width at half-maximum of the resonance curve.

This hydrodynamical treatment has been extended to deformed nuclei by Danos ⁹ and Okamoto ¹⁰. They show that if a nucleus is spheroidal in shape, it will exhibit two characteristic energies of resonance; E_b and E_a . Over the range of nuclear deformations, the splitting of eigenvalues is accurately given by ⁹:

$$\frac{E_b}{E_a} = 0.911 \frac{a}{b} + 0.089 \quad (2)$$

where a and b denote the length of the semimajor and semi-minor axis of the spheroid.

For splitting $E_b - E_a$ inferior to $\frac{1}{2} \Gamma$, the cross-section consists essentially of one broadened peak. If the splitting is greater than Γ , two peaks appear.

In a nucleus with positive quadrupole moment, $a > b$ and so the higher peak occurs at a higher energy. Conversely, in a nucleus with negative quadrupole moment, the higher peak occurs at a lower energy.

2. THE QUADRUPOLE MOMENT

Among the experimental methods used for measurements of nuclear electric-quadrupole moment, the μ -atomic hyperfine structure method is the most accurate. The μ -mesonic atom has proved to be a useful tool for measurements of nuclear size and shape. The reasons for its utility as a probe for nuclear electro-magnetic effects are well summarized by Wheeler ^{11, 12}, who emphasizes the smallness of the Bohr orbits and the transparency of nuclear matter to μ -mesons. Wheeler pointed out that from measurements of μ -mesonic X-rays, the shape as well as the extent of the nuclear charge distribution could be determined for nuclei with nuclear spin $I = 1$ and muon orbits with $j = 3/2$. Wilets ¹³ and Jacobson ¹⁴ reconsidered this problem, giving particular attention to highly deformed nuclei. Such nuclei have low-lying rotational states which give rise to novel effects. In the presence of the muon in a low-lying atomic state, the low rotational states mix with the ground state by quadrupole interaction. A complex hyperfine structure results, which appears even when the nuclear spin is zero or one-half.

and is detectable by means of a high resolution lithium-drift germanium. Such measurements of muonic X-rays serve to determine the intrinsic quadrupole moments of even-even nuclei and have been used for Th^{232} and U^{238} 3, 15.

Coulomb excitation experiments also provide information about quadrupole moment. The electric quadrupole reduced-transition probability is measured by means of studies of the inelastic scattering events from low energy protons or heavier ion bombardment in which the nucleus is excited to one of the rotational levels. (See the review article by Alder et al. ¹⁶ about Coulomb excitation).

In giant resonance experiments, using a highly deformed nucleus, two closely spaced resonances occur, corresponding to the major and minor axis of the deformed nucleus. The spacing of the two resonances is related to the quadrupole moment. However, since the resonances take place at high energies (above 10 MeV), the dynamic quadrupole associated with highly excited nucleus states is the quantity that is really measured.

The results of a few measurements of electric quadrupole moments are summarized in Table 1.

TABLE 1

	U^{238} : $Q_0(10^{-24} \text{ cm}^2)$
Coulomb excitation: half life (17)	10.52 ± 0.48
Coulomb excitation: cross-section (17)	11.25 ± 0.25
Coulomb excitation: conversion electrons (18)	11.5 ± 0.9
Muonic x-rays (16)	11.25 ± 0.15
Muonic x-rays (3)	11.47 ± 0.13

3. NUCLEAR PARAMETERS

The intrinsic quadrupole moment Q_0 of a spherioid nucleus is expressed by:

$$Q_0 = \frac{2}{5} Z R_{eq}^2 \varepsilon \quad (3)$$

where the nuclear radius

$R_{eq} = R_0 A^{1/3}$, is the radius of the equivalent uniformly charged spherical nucleus and a simple calculation shows that:

$$R_{eq} = \frac{1}{3} [(b^2 + 2a^2)]^{1/2} \quad (4)$$

ε is the nuclear excentricity given by:

$$\varepsilon = \frac{\eta^2 - 1}{\eta^{2/3}} \quad (5)$$

where the parameter η is the ratio of the major axis a to the minor axis b for a prolate nucleus.

The nuclear-symmetry energy for prolate deformed nuclei is calculated from the relation:

$$K = 9935 \times 10^{-4} (A^{8/3} NZ) \times \frac{|E_a|^2}{1 - [\Gamma_a/2\Gamma_a]^2} \times \frac{\eta^{4/3}}{(1 + 0.001860 \varepsilon - 0.3314 \varepsilon^2)^2} \quad (6)$$

Assuming the value of $(11.47 \pm 0.13) \times 10^{-24} \text{ cm}^2$ for the intrinsic quadrupole moment and for $R_0 = 1.2F$, we obtained the following results for the U^{238} :

TABLE 2

NUCLEUS	a (10^{-13} cm)	b (10^{-13} cm)	ϵ	η	K (MeV)
U^{238}	8.70	6.70	1.29	0.58	28.17

4. THE $U^{238}(\gamma, n)$ AND (γ, total) CROSS-SECTIONS

The thresholds of the $(\gamma, \text{fission})$, (γ, n) and $(\gamma, 2n)$ processes are respectively 5.0 MeV, 6.0 MeV and 11.5 MeV. The first giant-resonance peak is at 11 MeV, and up to 11.5 MeV, fission and (γ, n) are the only two competing processes. The fission cross-sections have been measured by Katz¹⁹ et al., and Duffield and Huizenga²⁰ have found the peak-energy of the (γ, n) cross-section curve at 11 MeV. We assume a width Γ for the $U^{238}(\gamma, n)$ cross-section curve of 2 MeV and a similar value was found by Bowman²¹ et al., for the $U^{235}(\gamma, n)$ cross-section curve. The contribution of the giant-resonance region to the (γ, n) cross-section per equivalent quantum (σ_q), (Measured at very high energies) is about 85% of the σ_q , and for that reason yields important information about the magnitude of the giant-resonance cross-section. The σ_q is given by:

$$\sigma_q(\gamma, n) = \int_0^{k_{\max}} n(k, k_{\max}) \sigma_k(\gamma, n) dk \quad (7)$$

where $n(k, k_{\max})$ represents the number of bremsstrahlung photons in the interval from k to $k + dk$, per energy unit; the

spectrum being normalized to one equivalent quantum. The integral in equation (7), at very high energies, is the sum of the contributions of three different processes: the giant-resonance up to 25 MeV, the quasi-deuteron and the photomesonic processes. The giant region, as has been mentioned, makes the most important contribution and therefore we can write equation (7) in the following manner:

$$\sigma_q(\gamma, n) = \int_0^{25} n(k, k_{\max}) \sigma_k(\gamma, n) dk + R. \quad (8)$$

It is possible to calculate the value of the remainder R , in two parcels. The first is the quasi-deuteron contribution process, with the cross-section expressed by the equation:

$$\sigma_k(\gamma, n) = 10 \frac{NZ}{A} \sigma_d T_n (1 - T_p) \quad (9)$$

T_n and T_p are neutron and proton nuclear transparencies and σ_d the cross-section for the photo-desintegration of the free deuteron. The contribution of the quasi-deuteron processes to the cross-section per equivalent quantum for U^{238} at 1000 MeV is 12 mb. The second part of the remainder arises from the mesonic processes beginning at 150 MeV. The photomesonic (γ, n) process cross-section can be calculated by means of a simple optical-photomesonic model and its contribution to the cross-section per equivalent quantum at 1000 MeV is only 8 mb, in

agreement with our experimental measurements.

At Frascati and DESY we have measured the $\sigma_q(\gamma, n)$ as function of energy for U^{238} from 300 MeV up to 6 GeV. We found for σ_q , by the least square method, a value of 158 ± 8 mb at 1000 MeV (Figure 1).

By subtraction of the remainder R equal to 20 mb from σ_q equal to 158 mb, the giant resonance part corresponds to 138 ± 8 mb.

Now, with the following boundary conditions: a width of 2 MeV, a threshold of 6.0 MeV and a maximum at 11 MeV, we found a Lorenz-line which satisfy a 138 mb contribution to σ_q for the integral $\int_0^{25} n(k, k_{\max}) \sigma_k(\gamma, n) dk$. This (γ, n) cross-section curve shows a maximum at 11 MeV of 400 ± 40 mb (Figure 2). Adding the Katz¹⁹ et al., photo-fission cross-sections to the $\sigma(\gamma, n)$ we obtained the total cross-section curve as far as 11.5, with its maximum of 470 ± 44 mb at $E_a = 11$ MeV. (Figure 2).

The energy E_p of the second maximum was obtained straightforwardly by means of equation (2), where the (a/b) ratio was taken from the experimental value of the intrinsic electric-quadrupole moment. (See section 3). The result found for E_p was 14 MeV.

Okamoto²² calculated the widths of the photonuclear giant-resonance for nuclei as a function of the neutron number. From analysis of the experimental data he concluded a constant

width Γ_0 of 4.2 MeV for all closed-shell (spherical) nuclei and a variable width equal to $\Gamma = \Gamma_0 + \Delta\Gamma$ for the deformed nuclei. $\Delta\Gamma$, the width increase, is due to the deformation and is nearly equal to ΔE , the dipole resonance energy split. In figure(3) are shown calculated values of Γ as a function of the neutron number obtained by Okamoto²². For U^{238} , the width value is 6.2 MeV. However, in the heavy nucleus the intrinsic width Γ_0 is 3.8 MeV²³. With this value, Γ is 5.8 MeV.

From the Danos⁹ relation $\Gamma_b \sigma_b = 2 \Gamma_a \sigma_a$ (10) and a resonance width of 5.8 MeV we found $\Gamma_{b/2} = 5.8 - \Delta E - \Gamma_{a/2} = 1.8$ MeV. We fitted a Lorenz-line with a peak at $E_b = 14$ MeV, $\sigma_b = 520$ mb and a width of 3.6 MeV. (See Figure 2).

5. THE (γ , 2n) CROSS-SECTION

The ratio of (γ , 2n) to the total cross-section was derived by Weiskopf from the Fermi gas model and is expressed by:

$$\frac{\sigma(\gamma, 2n)}{\sigma(\gamma, \text{total})} = 1 - \left(1 + \frac{E_c}{\theta}\right) \exp\left(-\frac{E_c}{\theta}\right), \quad (11)$$

where

$$\theta = \frac{(E_c - E_n)^{\frac{1}{2}}}{a} \quad \text{and} \quad E_c = E - E_{2n}$$

E_n and E_{2n} are the thresholds for the (γ , n) and (γ , 2n) processes, and a is the level density parameter in units of MeV^{-1} .

Equation (11) was applied to U^{238} , assuming a level density parameter a equal to 20 MeV^{-1} .

For comparison, figure (4) shows the $(\gamma, 2n)$ curves (---) for $a = 20 \text{ MeV}^{-1}$ and the solid line obtained by the subtraction of $\sigma(\gamma, f)$ and $\sigma(\gamma, n)$ from the total cross-section. The small disagreement between the calculated curves and the curve found by us, is probably due to the effect of fission competition with the $(\gamma, 2n)$ process.

6. THE (γ, N) CROSS-SECTION

The (γ, N) cross-section was obtained by the following relation:

$$\sigma(\gamma, N) = \sigma(\gamma, n) + 2 \sigma(\gamma, 2n) + \bar{\nu}(E) \sigma(\gamma, f) \quad (12)$$

where the $\bar{\nu}(E)$ is the average number of prompt neutrons emitted as a function of the photon energy. The $\bar{\nu}(E)$ dependence chosen was that of Condé and Holmberg²⁴ i.e.

$$\bar{\nu}(E) = 2.00 + 0.15 E \quad (13)$$

where E is the photon energy and 2.00 the average number of prompt neutrons from spontaneous fission. Figure (6) shows the total neutron emission cross-sections $\sigma(\gamma, N)$ for U^{238} , obtained in the present work. The $\sigma(\gamma, N)$ curve has a peak value of 1236 mb at 14 MeV and a Γ value of 6.0 MeV. The integrated cross-section up to 25 MeV is 7.5 MeV barn.

7. DISCUSSION

The $\sigma(\gamma, \text{total})$ has been analysed by Eq.(1) with the restriction imposed by Eq. (10). The lower-resonance width Γ_a was equal to $\Gamma(\gamma, n)$ and E_a equal to the energy peak of the (γ, n) process, owing to the fact that the photofission cross-section increases very slowly and has its maximum at 14 MeV. The Γ_a found was 2.00 MeV and the peak energy $E_a = 11.00$ MeV. The maximum value of $\sigma(\gamma, n)$ satisfying restrictions imposed by σ_q (at 1.000 MeV) which are equal to 158 mb and an integral value equal to 400 mb, in excellent agreement with the value found by Gindler et al.²⁵. In a first approximation we assume that the compound nuclei throughout the giant resonance has the same shape as the cold nucleus, i.e., we used the electric quadrupole moment, measured by μ -mesonic X-rays of 11.5×10^{-24} cm² as the average quadrupole in the giant resonance. If the actual width of the resonance were 6.2 MeV, the average quadrupole would be 13.2 MeV. We chose a width of 5.8, because of the fact that all nuclei in the neighbourhood of Pb-208 have a width of 3.8 MeV, i.e., a $\Gamma_0 = 3.8$ MeV. This restriction leads to a $\Gamma_b = 3.6$ MeV and $E_b = 14$ MeV for the higher-energy resonance. The maximum of the $\sigma(\gamma, \text{total})$ second peak has a value of 520 mb. The total cross-section is shown in Fig. (2).

The Sum Rule of Thomas-Reiche-Kuhn is in good agreement with our result. For comparison, we have fitted the available data^{21, 23, 26, 27, 28, 29}, by the least square method (Fig. (5)), and the $\int_0^{25} \sigma dE = 3.33$ MeV barn is in excellent agreement

with the straight line found in the fitting.

The nuclear symmetry energy K was obtained by two methods. From Eq. (6) we found 28.2 MeV in excellent agreement with the average value of 27.4 found by Bramblett et al. ²⁷.

The K value calculated by means of the Migdal ³⁰ σ_{-2} integral was 23.6, which is also in agreement with a $K = 23$ MeV based on Green's ³¹ evaluation of the Weizsaker formula. The small difference between 28.2 and 27.4 MeV indicates a value of 10.8 MeV for E_a . The $\sigma(\gamma, 2n)$ cross-section was obtained by the relation $\sigma(\gamma, 2n) = \sigma(\gamma, \text{total}) - \{\sigma(\gamma, n) + \sigma(\gamma, f)\}$. For comparison, we utilized the Weisskopf ³² equation (11) with a parameter a equal to 20 MeV^{-1} . This value was determined by the relation ³³:

$$a = \frac{\pi^2}{4} \frac{A}{E_F} \quad (14)$$

where E_F (Fermi energy) was taken as 29.3 MeV ³⁴ for heavy nuclei like U^{238} . Such a value, calculated for the even-even nucleus U^{238} is not small, since for the odd-even nucleus U^{235} , Cameron ³⁵ found a value of 28.9 MeV^{-1} . The $\sigma(\gamma, N)$ cross-section has a peak value of 1236 mbarn at 14 MeV and a Γ value of 6.0 MeV.

For comparison with results from other measurements, the data is shown in table (3). The integral $\int_0^{25} \sigma(\gamma, N)dE$, obtained by Fultz et al. ²¹, for U^{235} , is 19% larger than the one found by us for U^{238} . The U^{235} has a relatively

large fast-neutron fission factor, therefore the yield of bremsstrahlung photon neutrons from U^{235} , used as pulsed neutron sources, is at least 19% larger than from U^{238} .

TABLE 3

U^{238} characteristic of the giant resonance related to the total neutron emission cross-section (γ, N)

σ_{\max} (barns)	$E(\sigma_{\max})$ (MeV)	Half Width (MeV)	$\int \sigma dE$ (MeV - barns)	Ref.
-	15.8	7.1	-	(36)
1.8	13	5	11.4 (0-27.5)	(37)
0.96	14	6.4	7.1 (0-25)	(38)
1.18±0.15	14.9	6.8	12.9±1.0(0-28)	(39)
1.29	15.2	6.4	9.74	(40)
1.236	14.0	6.0	7.5 (0-25)	Present work

* * *

ACKNOWLEDGEMENTS

The authors wish to thank Dr. K. Tesch for the DESY data, and the Machine Group of the Synchrotron-Laboratory of the "Laboratori Nazionali di Frascati" for their assistance during irradiations. H. G. de Carvalho and J. B. Martins wish to thank the Brazilian "Conselho Nacional de Pesquisas" and the "Comissão Nacional de Energia Nuclear" for their financial help.

FIGURE CAPTIONS:

Fig. 1 - Cross-sections per equivalent quantum for $U^{238}(\gamma, n)$ and $U^{237} \sigma_q$ plotted against natural logarithm of the bremsstrahlung peak energy. The value of σ_q at 1000 MeV is 158 ± 8 mb.

Fig. 2 - The compound nucleus formation cross-section $\sigma(\gamma, \text{total})$ and the disexcitation processes $\sigma(\gamma, n)$, $\sigma(\gamma, 2n)$ and $\sigma(\gamma, f)$.

The dashed line - - - - represents the Lorenz-line of $\sigma(\gamma, n)$ with a maximum at 11 MeV and $\sigma_{\text{max}}(\gamma, n)$ of 400 ± 40 mb; dotted line represents the photofission cross-section $\sigma(\gamma, f)$ measured by Katz¹⁹ et al.; solid line _____ is the $\sigma(\gamma, 2n)$ cross-section obtained by subtraction of $\sigma(\gamma, f)$ and $\sigma(\gamma, n)$ from the total cross-section; dash-dotted line -.-.-.-.- represents the $\sigma(\gamma, \text{total})$.

Fig. 3 - The figure shows the calculated values of photon-nuclear resonance width Γ as function of the neutron number [Okamoto²²].

Fig. 4 - The dash-dotted line represents the curve $\sigma(\gamma, 2n)$ as function of photon energy, obtained by Weiskopf equation (11), with a level density parameter a equal to 20 MeV^{-1} ; the solid line _____ is the $\sigma(\gamma, 2n)$ obtained by subtraction of $\sigma(\gamma, f)$ and $\sigma(\gamma, n)$ from the total cross-section.

Fig. 5 - The dash-dotted line represents the Thomas-Reiche-Kuhn sum rule

$$\int_0^{\infty} \sigma(\gamma, \text{total}) dE = 0,06 \frac{NZ}{A} .$$

The solid line was obtained by the least square fitting of the available data ^{21, 23, 26, 27, 28, 29} for the integrated cross-sections, plotted against $\frac{NZ}{A}$. The point marked with Δ represents an integrated cross-section value of 3.3 MeV.b, for the Uranium ²³⁸, used in the present work.

Fig. 6 - Total neutron emission cross-section $\sigma(\gamma, N)$ for U^{238} as function of photon energy. This curve was obtained from the relation

$$\sigma(\gamma, N) = \sigma(\gamma, n) + 2\sigma(\gamma, 2n) + \bar{\nu}(E) \sigma(\gamma, f) . \quad (12)$$

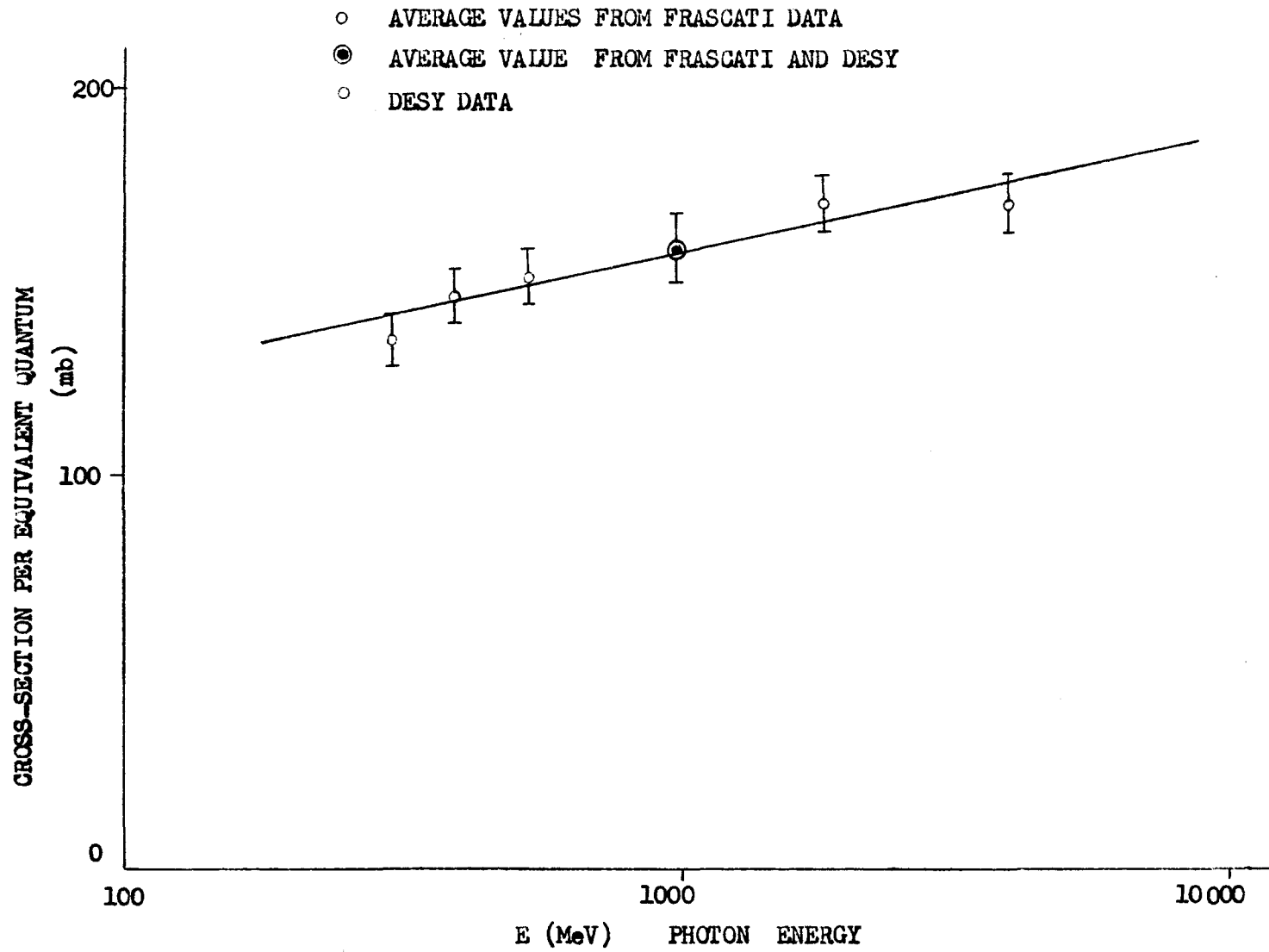


FIG. 1

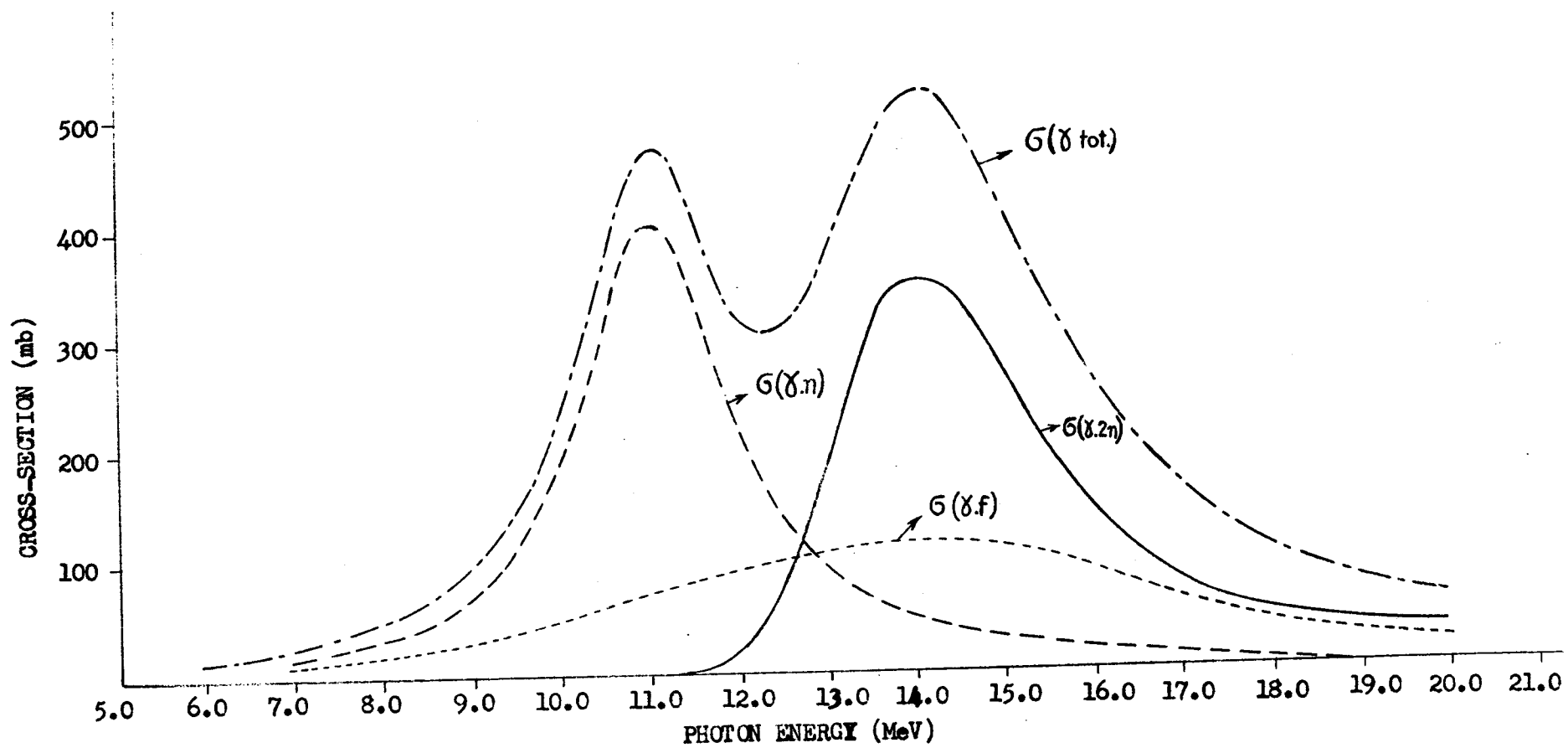


FIG. 2

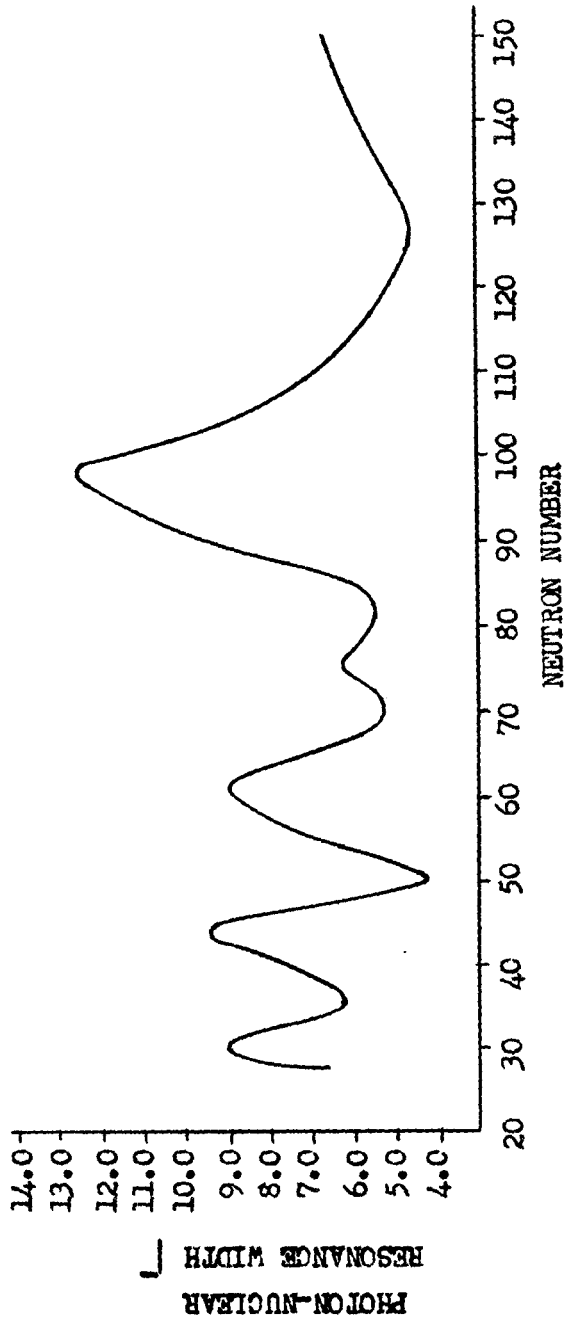


FIG. 3

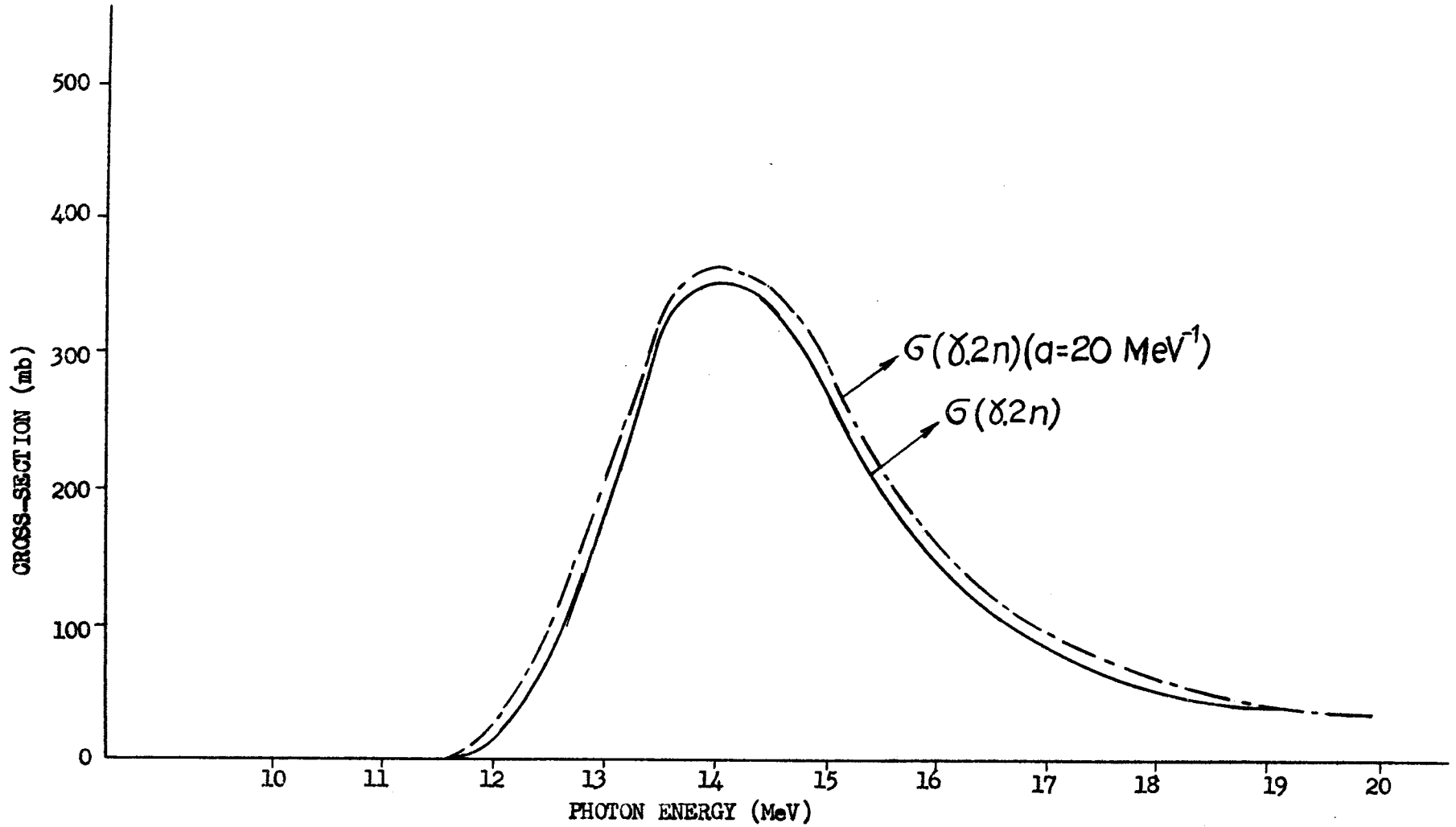


FIG. 4

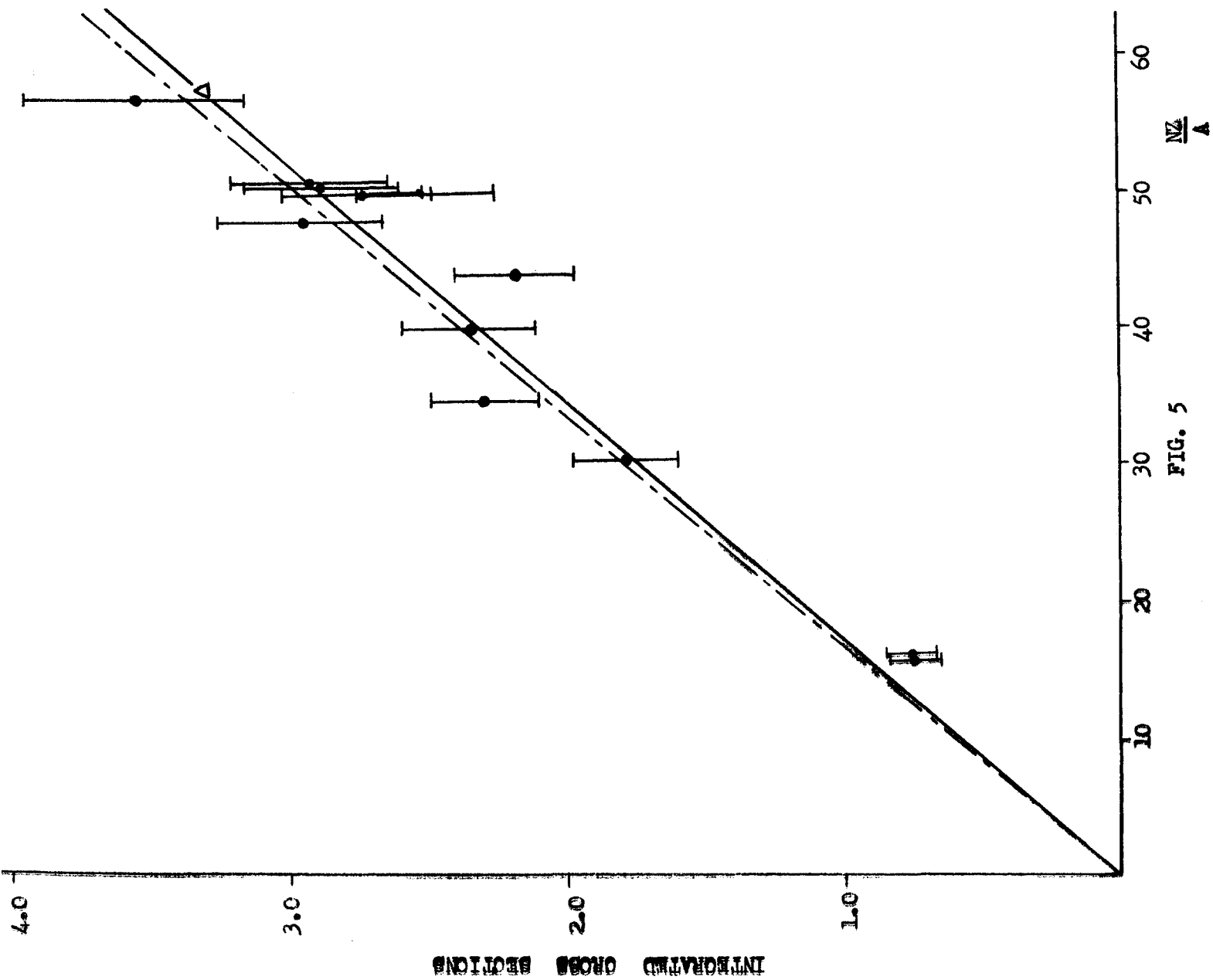


FIG. 5

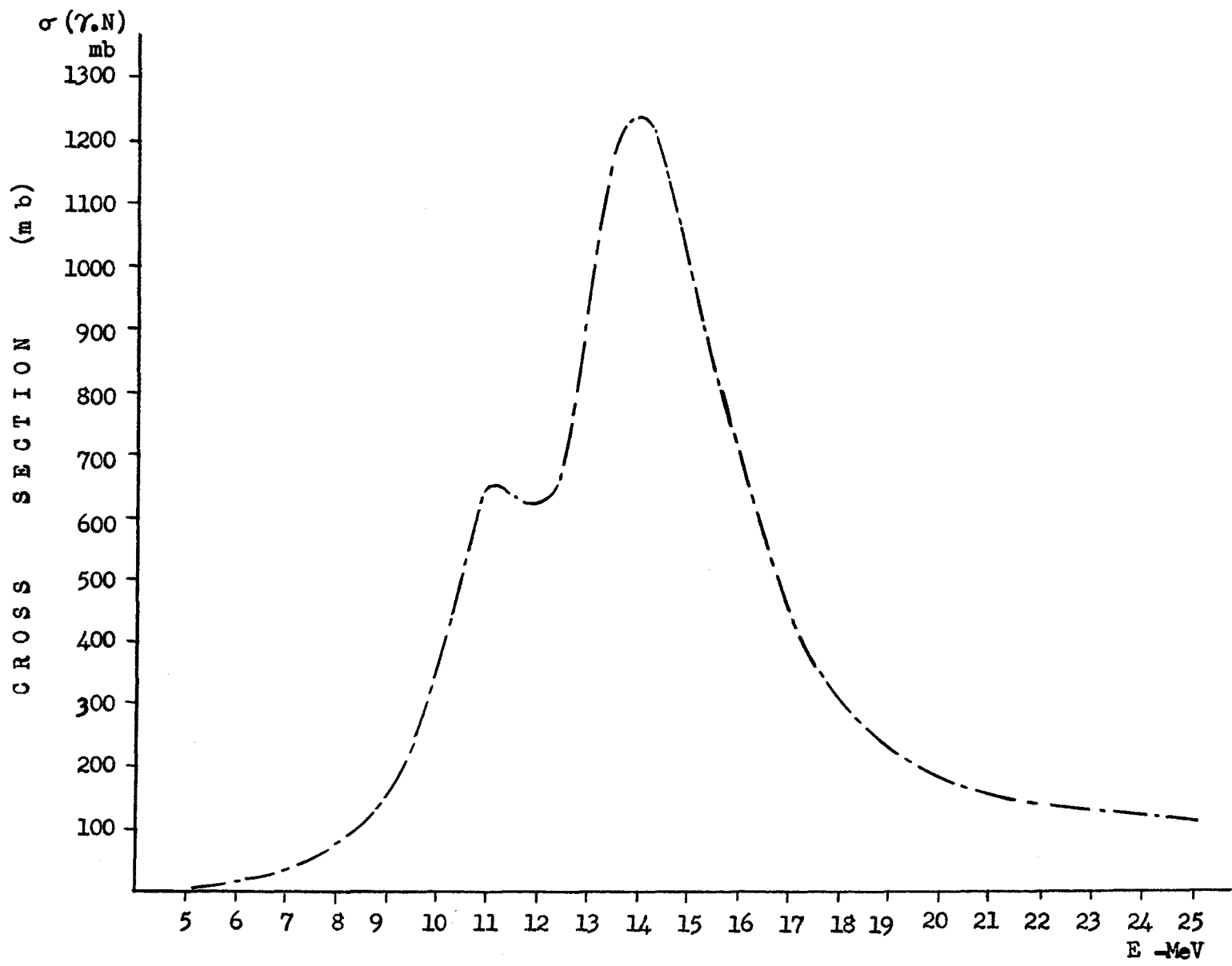


FIG. 6

REFERENCES:

1. H. G. de Carvalho, V. Di Napoli, D. Margadona, F. Salvetti and K. Tesch, Nuclear Physics A126, 505-512 (1969).
2. V. Di Napoli, D. Margadona, F. Salvetti, H. G. de Carvalho, J. Bemuzzi Martins, Gamma-neutrons reactions in Uranium-238 at Energies between 0.3 GeV and 1.0 GeV (to be published).
3. Robert J. McKee, Atomic Hyperfine Structure in the K, L and M Lines of U^{238} and Th^{232} , Department of Physics and the Enrico Fermi Institute - The University of Chicago, Chicago, Illinois, (1968).
4. J. H. D. Jensen and H. Steinwedel, Z. Natur Forsch 5a (1950) 413.
5. J. S. Levinger and D. C. Kent - Phys. Rev. 95 (1954) 418.
6. D. M. Brink, Nuclear Physics 4 (1957) 215.
7. M. Goldhaber and E. Teller, Phys. Rev. 74 (1948) 1046.
8. J. M. Araujo, Nuovo Cimento 12 (1954) 780.
9. M. Danos, Nuclear Physics 5 (1958) 23.
10. K. Okamoto, Prog. Theoret. Phys. (Kyoto) 15, (1956) 75.
11. J. A. Wheeler, Rev. Mod. Phys. 21 (1949) 133.
12. J. A. Wheeler, Phys. Rev. 92 (1953) 812.
13. L. Wilets, Dan. Mat. Fys. Medd. 29 No 3 (1954).
14. B. A. Jacobson, Phys. Rev. 96 (1954) 1637.
15. S. A. De Wit, G. Backenstoss, G. Daum, J. C. Sens and H. L. Acker - Nuclear Phys. 87 (1967) 657.
16. K. Alder, A. Bohr, T. Huus, B. Mottelson and A. Winther, Rev. Mod. Phys. 28 (1956) 432.
17. R. E. Bell, S. Bjornholm and J. C. Severiens, Mat. Fis. Medd. Dan. Vid. Selsk, 32 (1960) 12.
18. D. H. Rester, M. S. Moore, F. E. Durham and G. M. Glass, Nuclear Physics 22 (1961) 104.

19. L. Katz, T. M. Kavanaugh, A. G. W. Cameron and J. W. T. Spinks, Phys. Rev. 99 (1955) 98.
20. R. B. Duffield and J. R. Huizenga, Phys. Rev. 89 (1953) 1042.
21. G. D. Bowman, G. F. Auchampaugh and S. C. Fultz, Phys. Rev. 133 (1964) B 676.
22. K. Okamoto, Phys. Rev. 110-1 (1958) 143.
23. R. R. Harvey, J. Caldwell, R. L. Bramblett and S. C. Fultz, Phys. Rev., 136 (1964) B 126.
24. H. Conde and Holmberg - Proc. of the Symposium of Physics and Chemistry - Salzburg (1965) 93.
25. J. Gindler, J. R. Huizenga and R. Schmitt, Phys. Rev. 104 (1956) 25.
26. S. C. Fultz, R. L. Bramblett, J. T. Caldwell and R. R. Harvey, Phys. Rev. 133 (1964) B 1149.
27. R. L. Bramblett, J. T. Caldwell, B. L. Berman, R. R. Harvey and S. C. Fultz, Phys. Rev. 148 (1966) 1198.
28. R. L. Bramblett, J. T. Caldwell, G. F. Auchampaugh and S. C. Fultz, Phys. Rev. 129 (1963) 2723.
29. S.C. Fultz, R. L. Bramblett, J. T. Caldwell and N. A. Kerr, Phys. Rev. 127 (1962) 1273.
30. A. Migdal, J. Phys. U.S.S.R. 8 (1944) 331.
31. A. E. S. Green, Phys. Rev. 95 (1954) 1006.
32. J. M. Blatt and V. F. Weisskopf, Theoretical Nuclear Physics (John Wiley & Sons, Inc. New York, (1952)).
33. M. A. Preston, Physics of the Nucleus (Addison-Wesley Publishing Company, Inc. London, 1962).
34. E. Segre, Nuclei and Particles, (W. A. Benjamin, Inc. New York, 1964).
35. A. G. W. Cameron, Can. Journ. Phys. 36 (1958) 1040.
36. R. E. Anderson and R. B. Duffield, Phys. Rev. 85 (1952) 728.
37. L. W. Jones and K. M. Terwilliger, Phys. Rev. 91 (1953) 699.

38. R. Nathans and I. Halpern, Phys. Rev. 93 (1954) 437.
39. L. E. Lazareva, Gavrilov, B. N. Valuev, G. N. Zatsepina and V. S. Stravinsky, Conference of the Academy of Sciences of the U.S.S.R. (1955).
40. L. Katz, K. G. Mc Neil, M. Le Blanc and F. Brown, Can. J. Phys. 35 (19 7) 470.

* * *